

Chapter 7. SCIIB Pressure Sensor Performance Evaluations: Experiments, Results and Discussions

This chapter will summarize the experiments and results associated with the development of the single-mode fiber-based SCIIB pressure sensor system. We will start with the clarification of the most commonly used terms in terms of system specifications and performance characteristics. The complete evaluation includes the SCIIB signal processing unit characterization, SCIIB sensor probe evaluation, sensor system calibration, and system performance evaluations.

7.1 Definitions of the Performance Characteristics

A wide range of terms have been used to describe the essential performance characteristics of instruments and sensors. The most widely used terms include repeatability, accuracy, resolution, sensitivity, stability, dynamic range, linearity, zero offset, hysteresis, and frequency response. The use of these terms of specifications is certainly application related and should also take into account the environment in which the instrument or sensor is likely to operate. In many cases, there is a trade off between the specifications that can be achievable at a given cost. The intention of this section is to try to provide clear definitions for the terms used to define the SCIIB pressure sensor system performance.

Repeatability

The repeatability of an instrument is an indication of its ability to give the same results when it is used to measure the same quantity several times in succession under the same condition.

Accuracy

The accuracy is defined as the closeness of the agreement between the result of a measurement and the true value of the measurand. Often referred to as the error which is the indication of the measuring result of the instrument minus the true value of the measurement.

If an instrument has a poor repeatability, it would be also found to have a poor accuracy. But if it has a good repeatability, it does not necessarily mean that the instrument will have a good accuracy since it could be giving the same wrong answer all the time. If repeatability can be viewed as the ability to stick to the same story, accuracy is a measure of its ability to tell the truth. In general, a good repeatability depends on a good design and careful manufacture, whereas a good accuracy depends upon those two things plus a third: accurate calibration against a standard.

Resolution (Sensitivity)

Resolution or sensitivity of an instrument is defined as the minimum resolvable value of the measurand. From the user's point of view, it can be described as the instrument's ability to range of an instrument is defined as the largest range of the measured quantity that can be measured by the instrument within a specified accuracy.

Linearity

The linearity is defined as the departure of the calibration point from a straight line.

Hysteresis

The difference between outputs for a given pressure value under rising and falling heads. It can be significant when rapid level fluctuations are likely to occur.

Stability (Drift)

It is defined as the ability of an instrument to maintain the same specification within a specific length of time period (typically one year). The stability of an instrument is usually measured by the quantity of drift which is defined as the time dependent change in the characteristics of the instrument.

Dynamic error

Dynamic error is a measure of the instrument's performance under specified environmental conditions, especially in a temperature-changing environment. For example, the instrument can be tested in an oven to its full temperature range of operation. The error is often expressed in terms of the zero shift per degree Celsius ($^{\circ}\text{C}$).

Temperature coefficient

The percentage change in output per degree Celsius change in temperature. Sometimes, it is also called the temperature cross sensitivity.

Frequency response

This is a measure of the instrument's ability to track fluctuating measurement quantities. The frequency response of an instrument is defined as the maximum fluctuating frequency (or the minimum time) at which the measrand changes can be measured with a specific degree of accuracy.

7.2 Evaluation of the SCIIB Signal Processing Unit

In this section, we will concentrate on the evaluation of the SMF SCIIB instrumentation system (without the sensor probe). By separating the sensor probe from the SCIIB instrumentation, we will be able to isolate problems for future development work.

7.2.1 Evaluation of the self-calibration capability

The SCIIB technology can self-compensate for source power fluctuations and fiber loss variations by self-referencing the two channels output. To evaluate the self-calibration capability of the SCIIB signal processing method, we conducted an experiment using the developed SCIIB instrumentation system.

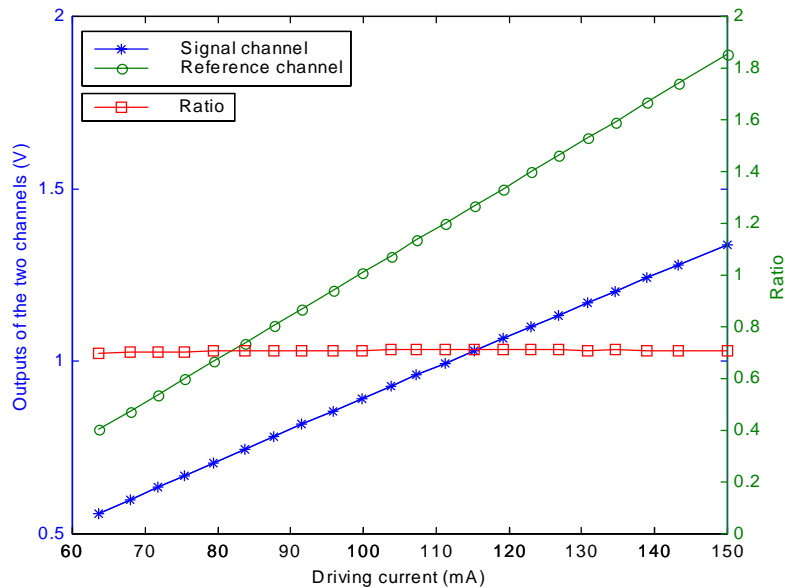


Figure 7-1. SCIIB outputs versus driving current of the optical source

Without connecting to the sensor probe connected to the system, the output power of the source (SLED) was changed by changing the driving current of the source chip. With the endface of the lead-out fiber well cleaved, the SCIIB instrumentation system should output a constant ratio though each channel's output could change when the total optical power was changed. In the experiment, two multimeters were used to record the two channels' output voltages. Then their ratio was calculated manually. Figure 7-1 plots the recorded two channels' outputs as well as their ratio with respect to the driving current of the light source.

Figure 7-2 shows the magnified change of the SCIIB ratio as a function of the normalized optical power of the source. As shown in the two figures, the ratio of the two channels only changes about 0.3% as the total optical power changes up to 50%.

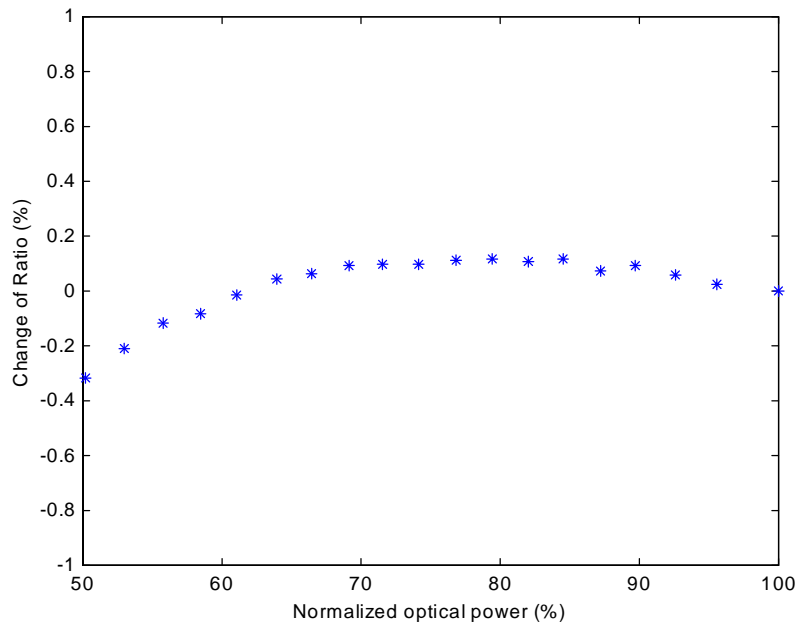


Figure 7-2. Change of SCIIB output ratio versus the normalized source power change

Theoretically, changing the drive current of a semiconductor optical source would also change the spectrum in addition to the optical power change. As discussed in Section 6.2.1, the distortion of the source spectrum would also introduce error to the measurement result through the non-centered filtering effect. Therefore, the error shown in Figure 7-2 has also indicated the contribution from the source spectrum distortion. Nevertheless, the experimental results reveal that the SCIIB signal processing has a good self-compensation capability as expected.

7.2.2 Evaluation of the polarization sensitivity

As proposed in Section 6.3, we used a fiber optic depolarizer to reduce the system sensitivity to the change of state of polarization due to fiber bending, which is unavoidable in actual fiber deployment.

To get an idea of how severe the polarization state would affect the system performance, we first test the SCIIB instrumentation without the depolarizer. Again, the system was tested without the sensor probe and the signal was directly from the reflection of the fiber endface. To change the SOP, we bent the fiber into a circle of different radii and flipped the fiber circle to different orientations. The SCIIB two channels' outputs were then recorded using an oscilloscope as shown in Figure 7-3. The ratio of these two outputs are plotted in Figure 7-4. As we see, the two channels' outputs were sensitive to the change of SOP, and moreover, they did not follow each other due to the polarization effect. The peak-to-peak variation in this case was about 5% of the average ratio.

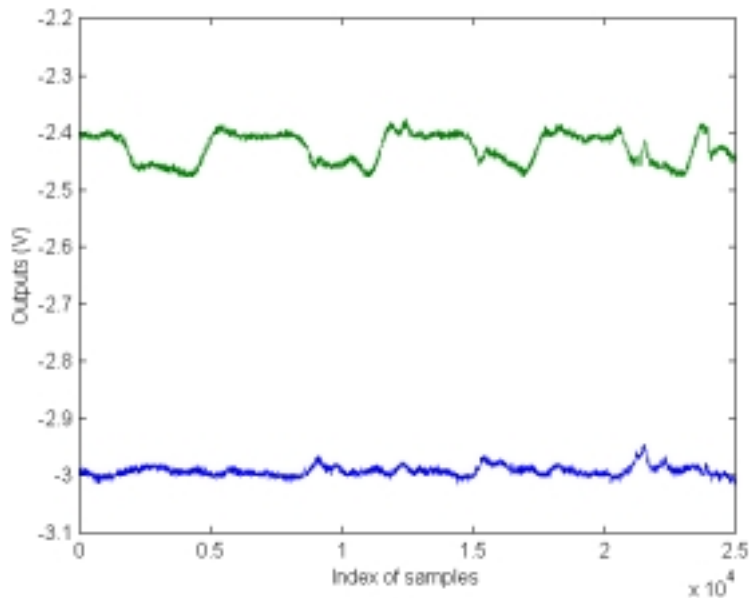


Figure 7-3. SCIIB two channels' outputs as SOP of the fiber changes (without the depolarizer)

The experiment was conducted again with the depolarizer connected to the system. The two channels' outputs are shown in Figure 7-5, and their ratio is shown in Figure 7-6. With the fiber optic depolarizer, the two outputs followed each other very closely. The maximum variation of the ratio was reduced to about 0.5%, showing an improvement of one order of magnitude.

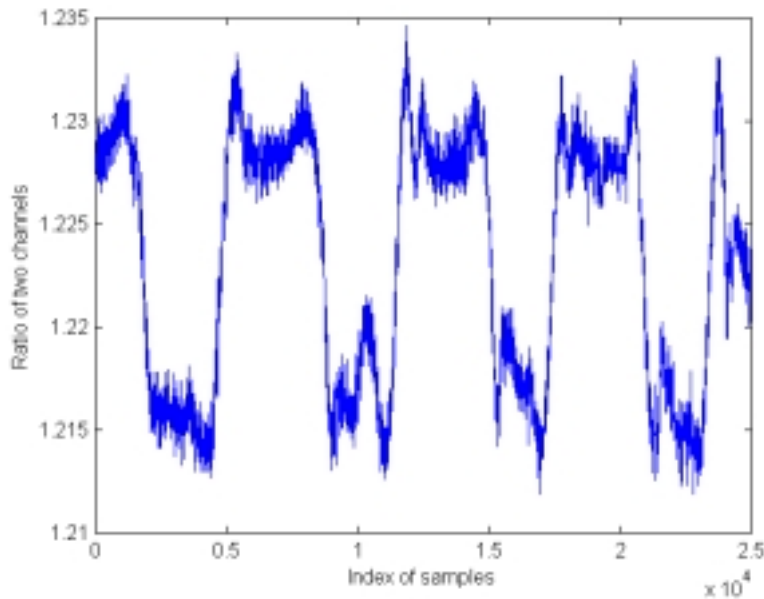


Figure 7-4. Ratio of the SCIIB two channels' outputs as SOP of the fiber changes (without the depolarizer)

However, the experiment also indicated that the dependence of the SCIIB ratio was still large compared to the analytical prediction given in Section 6.2. The fiber optic Lyot depolarizer purchased from Noah Industries, Inc. was tested using a wide-spectrum light source. The optical bandpass filter used in the system had a spectral width of 10nm, which was narrower than the spectral width of the light source that had been used to test the depolarizer. The specified 20dB extinction ratio of polarization suppression might not be true for the signal channel. Therefore, we would expect to have larger polarization dependence of the SCIIB output ratio than the analytical prediction.

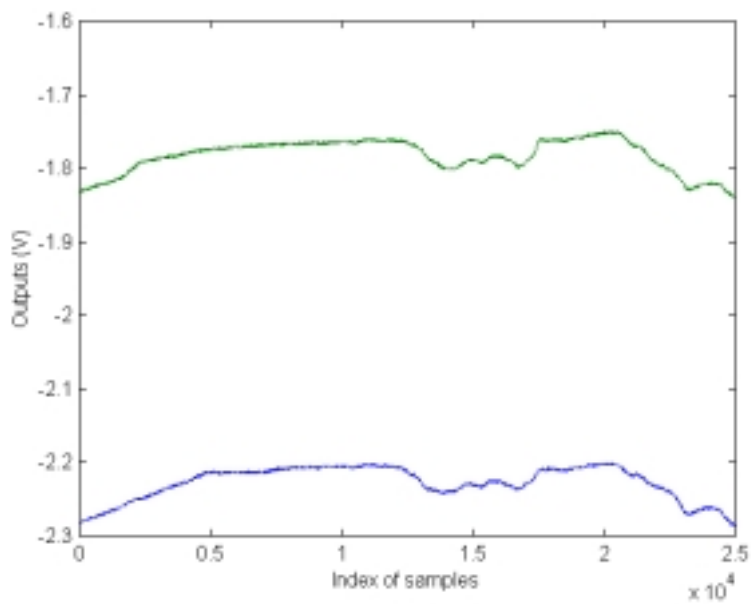


Figure 7-5. SCIIB two channels' outputs as SOP of the fiber changes (with the depolarizer)

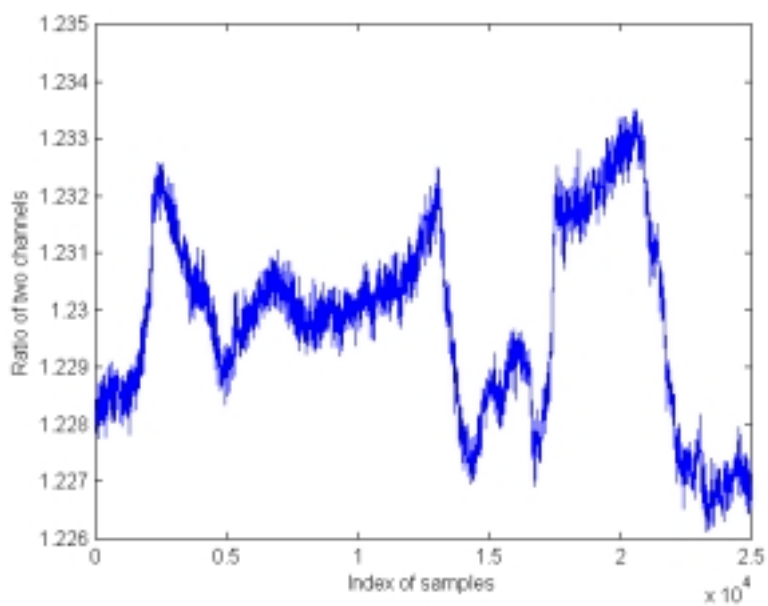


Figure 7-4. Ratio of the SCIIB two channels' outputs as SOP of the fiber changes (with the depolarizer)

7.2.3 Dynamic error of the SCIIB instrumentation

The change of the environmental temperature could have multiple effects on the SCIIB instrumentation system. As discussed in the last chapter, the spectrum of the light source, the spectral characteristics of the optical bandpass filter, the beamsplitter, the amplifiers and the photodetectors are all temperature dependent. The change of the environmental temperature will eventually cause measurement errors.

Experiments were also conducted to evaluate the dynamic error of the developed SCIIB instrumentation system. Again, the system was not connected to the sensor probe and just took the reflection from the fiber endface as the signal. In the experiment, the SCIIB system was put in an electronic oven. A thermal couple was placed inside the oven to record the actual temperature inside the oven. The oven was then heated up to 57°C stabilized for about half an hour. Then the oven was shut down. During the period that the temperature inside decreased slowly, the SCIIB two channels' outputs were recorded using two multimeters every degree Celsius from 57°C to 20°C. The recorded outputs are plotted as shown in Figure 7-7, with their ratio shown in Figure 7-8. As shown in Figure 7-7, the outputs of the two channels changed as the environmental temperature changed. However, the two channels followed each other in the same direction. The change of their ratio was within 1% within the testing temperature range of 37°C. The dynamic error of the SCIIB instrumentation system is about 0.027%/°C.

Due to the limitation of the experimental equipment, we could not create environmental temperature changes lower than the room temperature. However, the above-mentioned experimental results mentioned above make us believe that the SCIIB instrumentation system could maintain its accuracy of a few percent of the full scale within the specified temperature range of operation. Moreover, the instrumentation is usually placed in a control room with a relatively small fluctuation of the environmental parameters. The actual dynamic error will then be far smaller.

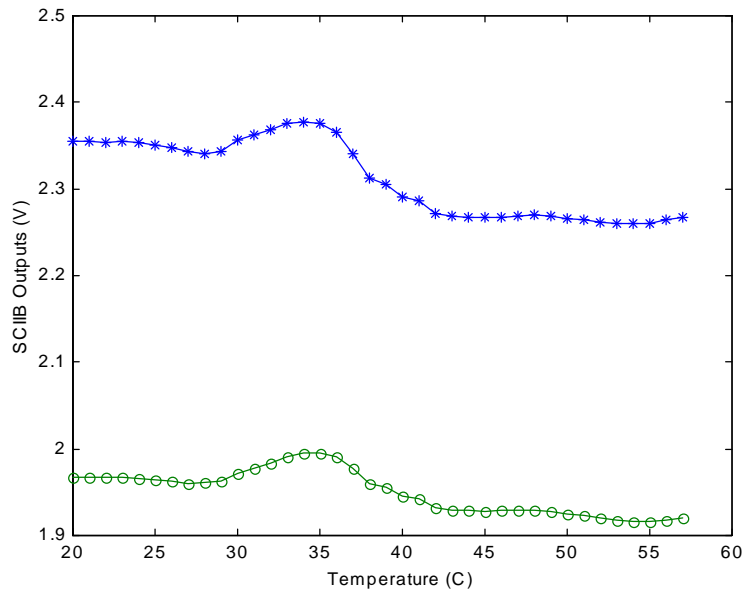


Figure 7-7. SCIIB instrumentation dynamic error test (two channels' outputs)

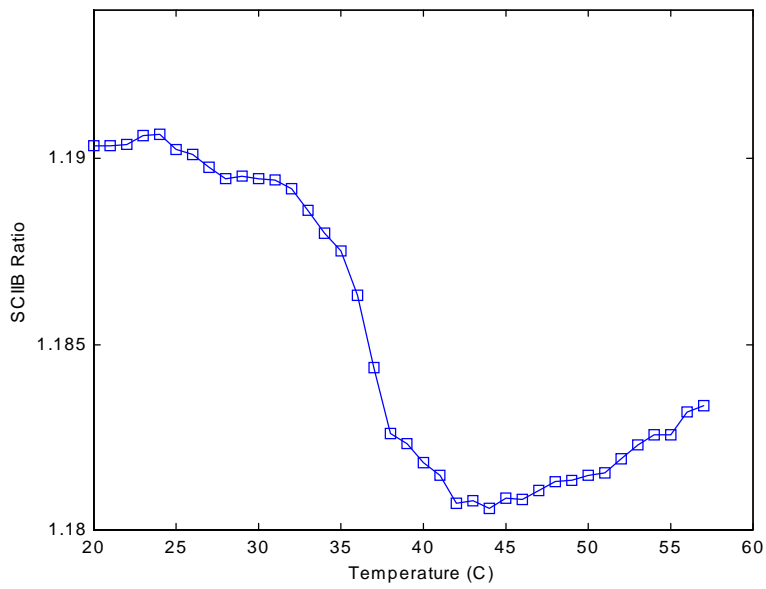


Figure 7-8. SCIIB instrumentation dynamic error test (SCIIB ratio)

7.3 Evaluation of the SCIIB sensor probe

As discussed in Chapter 4, the SCIIB sensor probe is fabricated using the controlled thermal bonding method, by which the silica glass fibers are fused with the fused silica glass capillary tube. Therefore, the sensor probe is expected to have a strong mechanical strength and can sustain high pressures. The sensor temperature model given in Chapter 5 also reveals that the SCIIB pressure sensor has very small temperature dependence. Experiments were conducted to evaluate the sensor's survivability and temperature dependence.

7.3.1 Survivability of the sensor probe

Up to date, hundreds of SCIIB sensor probes have been made using the developed fabrication system. Before the sensors can be used in harsh environments, they must be tested to ensure a complete sealing at the two fusion points because an imperfect sealing would result in the intrusion of the outside medium and degradation of the sensor performance. More than one hundred sensors were first tested in the water environment of high pressure (>3000 psi) and high temperature (>200°C). So far, only two sensors were found to leak water into the cavities during the test. The majority of the sensors successfully survived the test. This made us believed that the controlled thermal bonding method could provide sensor probes strong enough to survive in harsh environments.

7.3.2 SCIIB sensor annealing

The capillary tube and glass fibers are fused together in a very short time period during the sensor fabrication process. It will be a reasonable concern about the residual stresses left built in the bonding regions due to the very large temperature difference. These residual stresses, when they release slowly, will cause sensor to drift from its original

calibrated operating point. Therefore, the sensor must be properly annealed to release the built-in stresses prior to sensor calibration.

The sensor annealing was done using an electrical furnace at a temperature of 600°C for 24 hours. During the annealing process, the temperature was increased and decreased slowly to avoid further stress built in. In order to see how the annealing affects on the sensor, five sensors were annealed twice under the same experimental condition, and the cavity lengths of the five sensors were monitored using the whitelight interferometer during the entire annealing process. The recorded changes of the cavity lengths are listed in Table 7-1.

Table 7-1. Sensor cavity length change before and after annealing

Sensor index	Gauge Length (mm)	Cavity length before annealing (μm)	Cavity change first annealing (nm)	Cavity change second annealing (nm)
1	0.7	20.0872	-37.2	2.7
2	1.0	39.6614	-15.8	3.3
3	1.0	29.1794	-68.4	*
4	1.0	20.4749	-32.2	1.9
5	0.7	21.3901	-13.1	3.4

*The sensor was broken after the first annealing because of mishandling.

As shown in the table, the changes of the sensor cavity lengths after the second annealing became very small compared to the first one, which indicate that the annealing process did improve the stability of the sensor. Although the sensors used in the experiment were chosen with different parameters (gauge lengths and initial cavity lengths) in hope to find the regularity of the annealing effect on the sensors, the results shown in Table 7-1 did not indicate an obvious relationship between the sensor parameters and the changes of

cavity lengths except that all the sensors showed a decrease in their cavity lengths after the annealing process. Nevertheless, the experiment indicated that the annealing process did cause a large change of the sensor cavity length with respect to the linear range of operation (about 200nm). Therefore, the sensor annealing is proved to be necessary to assure the performance of the sensor.

7.3.3 Temperature dependence of the SCIIB sensor probe

The temperature model of the SCIIB sensor probe has been given in Chapter 5, where the analysis showed that the temperature sensitivity depends on the sensor gauge length, the initial cavity length, and the CTEs of the fiber and the capillary tube. It is possible to design the sensor according to the temperature model to have very small or even zero temperature sensitivity.

The actual CTEs of the fiber and the tube can deviate from the nominal values due to the small difference in the chemical composition among the materials used by different manufacturers. It is very difficult to determine the actual temperature dependence of the sensor probe by just referencing the nominal CTEs due to the extremely high accuracy required. The actual temperature dependence of the sensor probe therefore has to be measured experimentally.

1. Multimode SCIIB sensor probe

The experimental set-up included an electric furnace with its maximum temperature up to 1100°C and an Omega CN76000 thermometer to read the temperature with an accuracy of 0.1°C. The multimode sensor probe and the thermocouple were put side by side in the furnace, and the temperature was increased from room temperature (30°C) to 810°C in steps of 10°C. Both the SCIIB sensor output and the thermometer output were recorded for comparison.

The capillary tube used to fabricate the multimode sensor was made of fused silica purchased from Polymicro Technologies, Inc. The inner diameter of the tube is 130 μm , and the outer diameter is 365 μm . The sensor had an effective gauge length of 0.7 mm, and the initial cavity length of 5.160 μm . The sensor output versus the increase of the temperature is plotted in Figure 7-9.

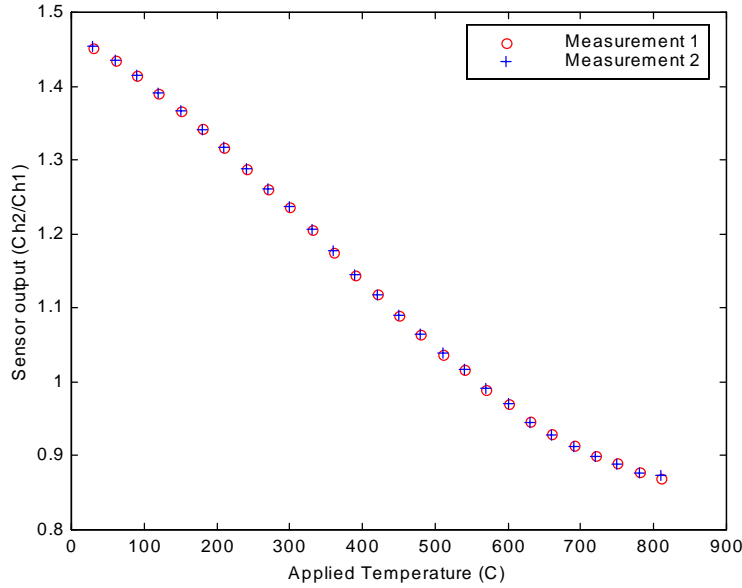


Figure 7-9. Multimode SCIIB sensor temperature sensitivity test result

As shown in Figure 7-9, the SCIIB system output was estimated to cover about 70% of the change from the peak to the valley of an interference fringe when the temperature changed from 30°C to 810°C. It was known that half of the interference fringe corresponded to a sensor cavity length change of a quarter of the central wavelength. Therefore, with the source central wavelength of 850 nm, the temperature sensitivity of the multimode sensor could be estimated by the following equation

$$s_{t,m} = \frac{70\% \times \frac{1}{4} \times 850[\text{nm}]}{(810 - 30)[^\circ\text{C}] \times 0.7[\text{mm}]} = 2.7 \times 10^{-7} \left[\frac{1}{^\circ\text{C}} \right]. \quad (7-1)$$

Although the temperature sensitivity given in Equation (7-1) is only an estimate, the result agrees with what the temperature model predicts. The experimental results indicate that the multimode fiber-based sensor probe has a large temperature dependence compared to its linear operating range. This is mainly due to the large CTE of the fiber which results from the large quantity of dopants used to increase the core refractive index and fill the relatively large core. The large difference between the CTE of the fiber and that of the fused silica tube makes the multimode fiber-based sensor probe have a large temperature dependence. When the multimode fiber-based sensor is used for pressure measurement in harsh environments where the temperature variation could be large, the large temperature dependence can introduce an unacceptable error to the final result.

2. Single-mode fiber SCIIB sensor probe

Single-mode fibers have a smaller core diameter and refractive index difference compared to multimode fibers. The smaller amount of dopants in single-mode fibers makes the single-mode fiber have a CTE very close to that of fused silica, and hence less temperature dependent compared to the multimode fiber sensor.

To determine the actual temperature sensitivity of the single-mode fiber-based sensor probe and also in hope to find an optimal design of the sensor probe to achieve zero temperature dependence, we fabricated five single-mode fiber sensors and measured their temperature sensitivity experimentally. The parameters of these five sensors are listed in Table 7-1. The experiments were conducted using the same electrical furnace for the sensor annealing. Because the temperature sensitivity of the single-mode sensor is very low, it is almost impossible to increase the temperature high enough to cover one-half interference fringe as we did for the multimode fiber sensor. The whitelight interferometry was thus used to measure the sensor cavity length. Figure 7-10 shows the recorded sensor cavity lengths measured as the temperature inside the furnace increased from room temperature up to 650°C at the step of 50°C.

As shown in Figure 7-10, all the sensors showed a decrease in the cavity length as the temperature increased. Also, it was found that a shorter gauge length resulted in smaller temperature sensitivity. However, there was no obvious relationship between the initial cavity length and the temperature dependence, unlike what the temperature model given by Equation (5-6) predicted.

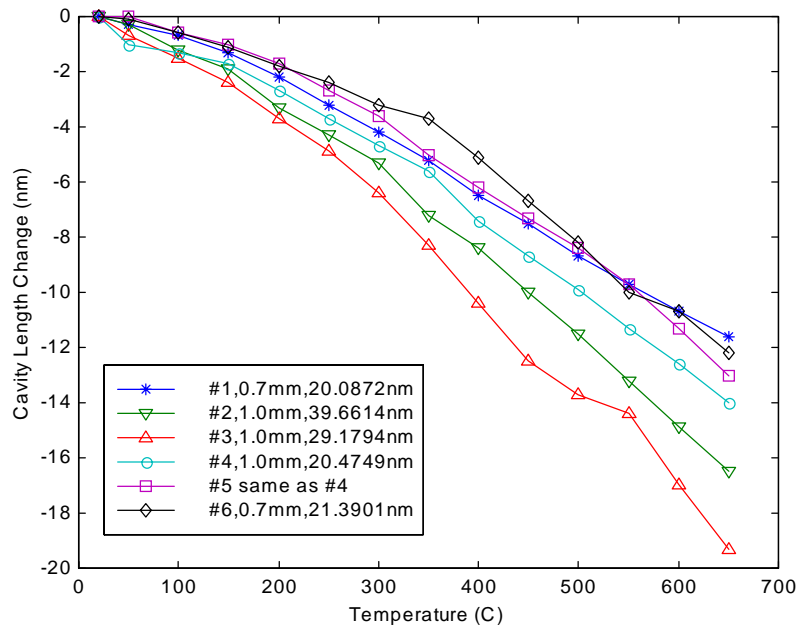


Figure 7-10. Temperature sensitivity test results of single-mode sensor probes

Although efforts were attempted to find the exact CTEs of the fiber and the capillary tube by solving the linear equations formed by the experimental data, the results conflicted with each other. The reason is believed to be that the accuracy of the whitelight interferometry was not high enough compared to the required resolution. In order to provide meaningful data for the equation solving to find the actual CTEs, a more accurate method for displacement measurement must be used. Nevertheless, the experimental data did provide some information of the temperature dependence of the sensor. For example, a sensor with a gauge length of 0.7mm (corresponding to 4000psi pressure measurement range), and an initial cavity length from 20 μ m to 30 μ m will have a temperature

sensitivity of $0.02\text{nm}/^{\circ}\text{C}$ (or $2.86\times 10^{-8}/^{\circ}\text{C}$), which is an order of magnitude lower compared to that of the multimode fiber sensors.

7.4 SCIIB pressure sensor calibration

Before the SCIIB sensor probe can be used for actual pressure measurement, it must be calibrated to relate the output ratio to the applied pressure. The sensor calibration is usually conducted by applying known pressures within its operating range. The one-to-one relation between the sensor original output and the applied pressure forms the calibration curve which can be stored in the host computer and later used to convert the sensor output to the pressure reading.

7.4.1 Construction of the Pressure Testing System

The sensor calibration system was constructed based on a computer-controlled high-performance pressure generator/controller manufactured by *Advanced Pressure Products, Inc.* The system configuration is shown in Figure 7-11. The pressure controller/generator can supply a hydrostatic pressure up to 20,000 psi, and the accuracy of the pressure output is 0.1% of the full scale. The construction of this system allowed us to precisely and automatically calibrate the SCIIB pressure sensor within its whole operating range. The system also allows us to test many performance characteristics of the SCIIB pressure sensor such as the linearity, hysteresis, repeatability, and dynamic range. In addition to these testing capabilities, several specially designed high temperature chambers were constructed by using heating tapes to heat the fluid and thermocouples to monitor the temperature inside. Using these chambers, the pressure sensors can also be tested at elevated temperatures.

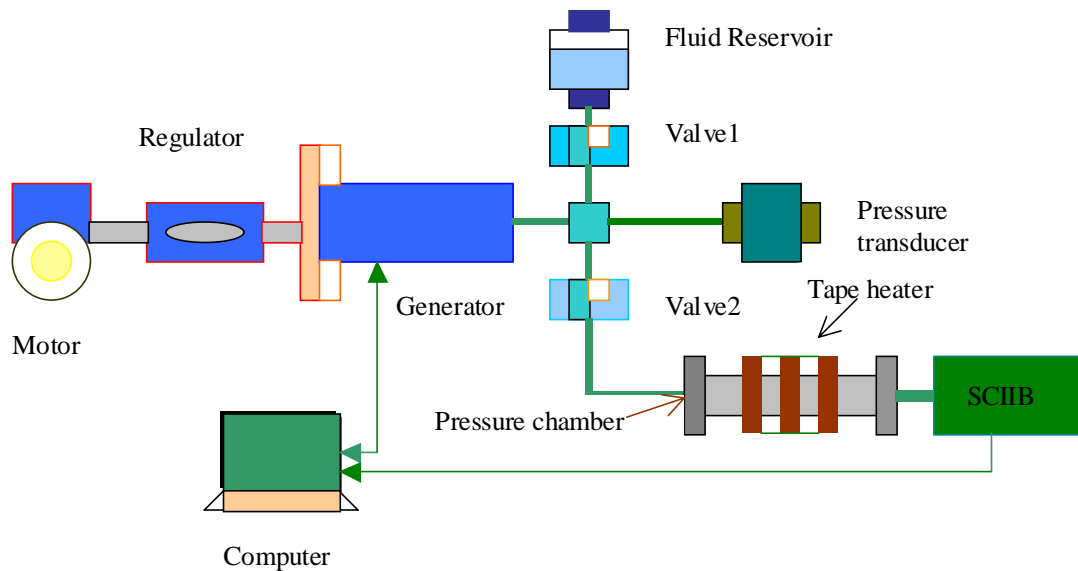


Figure 7-11. Schematic of APP pressure sensor test system

7.4.2 Pressure Sensor Calibration

During the calibration process, the pressure sensor was installed inside the pressure calibration chamber. Through the computer programs, the hydrostatic pressure was applied to the sensor at the increment of 1/40 of the estimated linear range of the pressure sensor. The pressure gauge inside the APP system measured the hydrostatic pressure inside the chamber and the system saved the data as applied pressure. At the same time, the output of the SCIIB system was sampled through the A/D converter and stored into another data file. To ensure the accuracy of the calibration, the system held the pressure at each step for about 50 seconds before moving to the next step. By taking the average within the pressure holding period, the error was minimized. Figure 7-12 shows the typical applied pressure data, and Figure 7-13 is the SCIIB output data recorded during the sensor calibration. The sensor used in the test was a single-mode fiber sensor with the gauge length of 0.5mm, the initial cavity length of 25.46 μ m, and the interference fringe

visibility of 70%. Figure 7-14 plots the SCIIB output versus the applied pressure after averaging. The one-to-one relation of the applied pressure and the SCIIB output was then used to find the calibration equation through polynomial fitting. Experimental results revealed that the optimal order of the polynomial fitting was 10. Usually, the calibration curve was obtained by taking the average of several consecutive calibration data to further ensure the accuracy of calibration.

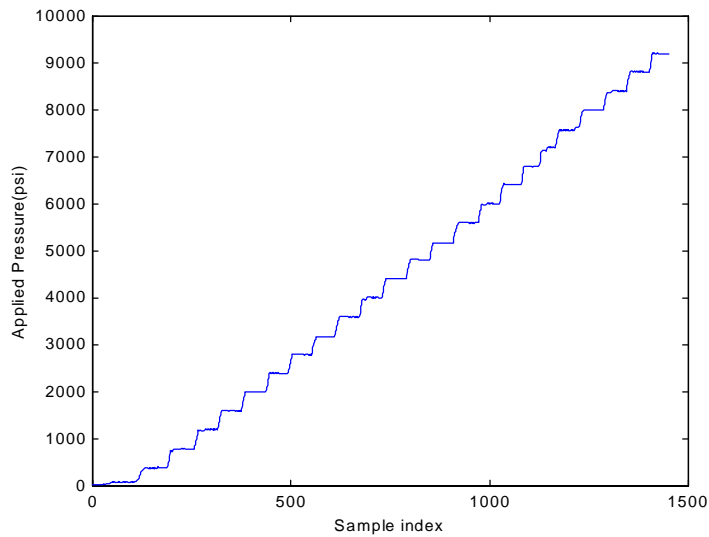


Figure 7-12. Applied pressure recorded during sensor calibration

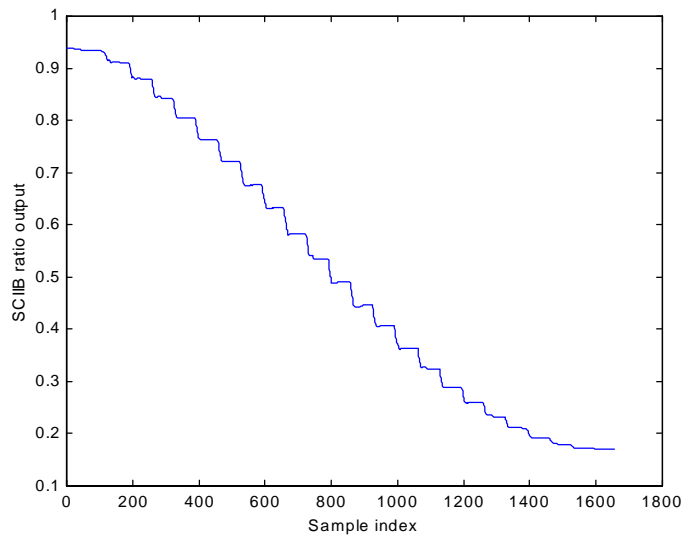


Figure 7-13. SCIIB output ratio recorded during the sensor calibration

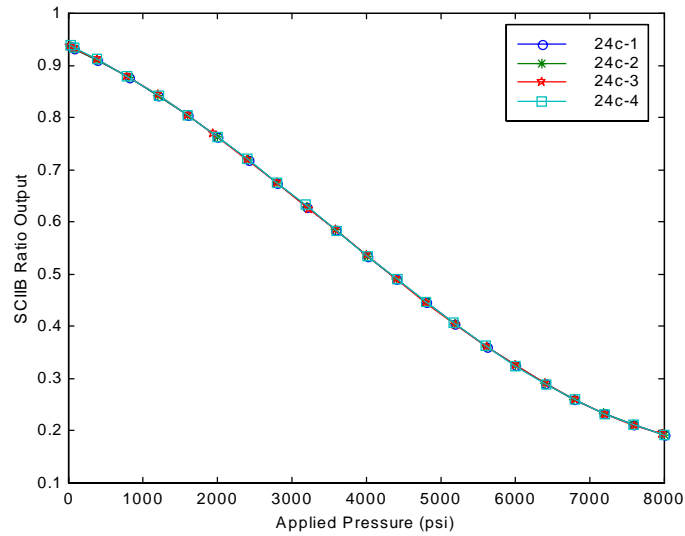


Figure 7-14. SCIIB pressure sensor calibration curve

7.5 SCIIB Pressure Sensor System Performance Evaluation

With a calibrated sensor, we are ready to evaluate the performance of the developed SCIIB pressure sensor system. The performance characteristics that have been evaluated so far include the linearity, hysteresis, resolution, repeatability, system stability, temperature cross sensitivity, and over pressure capability.

7.5.1 Linearity of the Sensor System

Due to the sinusoidal nature of the interference signal, the direct output from the SCIIB pressure sensor is a nonlinear function of the applied pressure. However, the calibration process can linearize the SCIIB output data by polynomial curve fitting. To assess the residual nonlinearity of the sensor system, we examined the measurement result after calibration, as shown in Figure 7-15, with respect to the applied pressure given by the APP system. The sensor used in the test was a single-mode fiber sensor with the gauge length of 0.5mm, the initial cavity length of 25.46 μ m, and the interference fringe

visibility of 70%. The magnified deviation between the calibration line and the straight line is plotted in Figure 7-16. As we see, the maximum deviation is about 9psi. If we normalized the nonlinearity with respect to its full dynamic range of 8500psi, the normalized nonlinearity error is less than 0.1% of the full scale of pressure measurements, which is the best accuracy offered by the pressure calibration system.

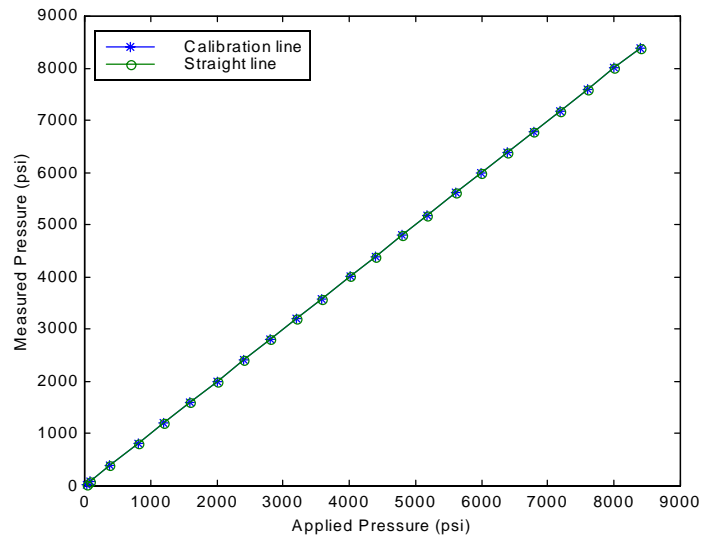


Figure 7-15. SCIIB pressure sensor system calibration lines

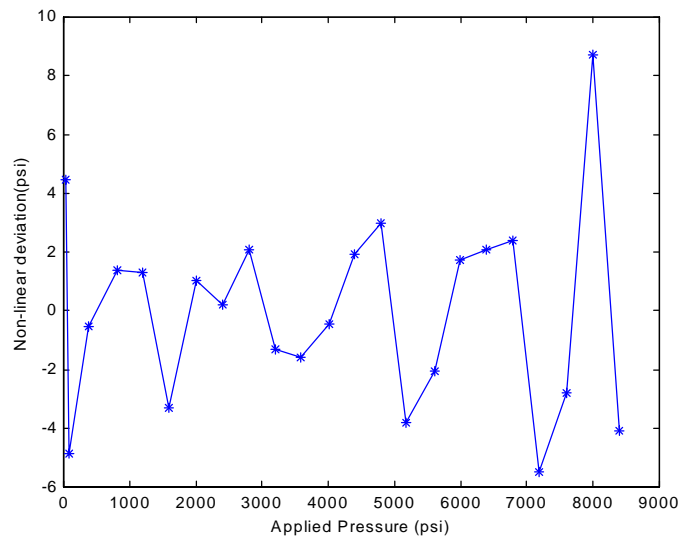


Figure 7-16. Nonlinearity of the SCIIB pressure sensor system

7.5.2 Hysteresis of pressure measurement

Hysteresis of the pressure sensor can be measured by cycling the applied pressure between the minimum and the maximum of the operating range in both increasing and decreasing directions. The hysteresis can be calculated as the largest difference among the output readings of the pressure cycles. The SCIIB pressure sensor probe is made of silica glass material and the operating range of the sensor in terms of pressure induced strain is very small. Therefore, the hysteresis of the sensor probe is expected to be very small. Nevertheless, experiments were conducted to evaluate the actual hysteresis of the SCIIB sensor probe. The evaluation was conducted using the *APP* pressure system after the sensor system was calibrated. The applied pressure was first increased to the maximum operating range of 8500psi at the step of 400psi. The pressure was then decreased to the atmosphere pressure after it was maintained at 8500psi for several minutes. The measurement results are shown in Figure 7-17. The experimental results confirm our expectation. There was no noticeable hysteresis found within the entire operating range.

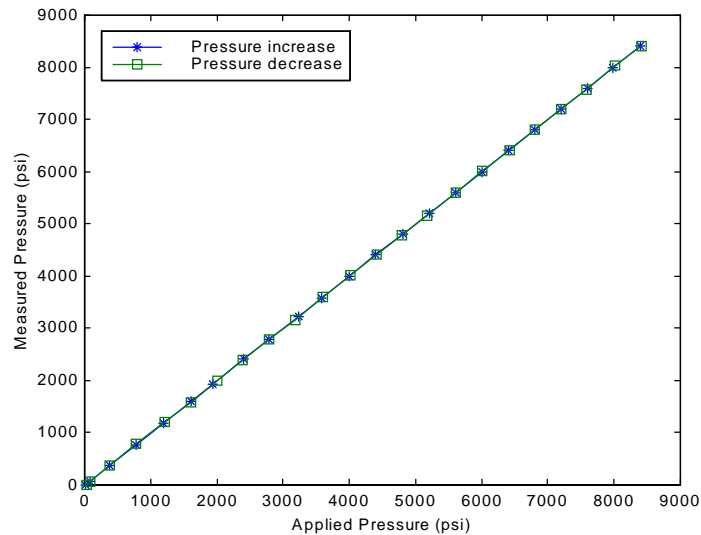


Figure 7-16. Hysteresis of the SCIIB pressure sensor

7.5.3 Resolution of pressure measurement

The resolution of the sensor system is usually interpreted by its standard deviation of a series of pressure measurements. It is common to use twice the standard deviation as the direct measure of resolution. The evaluation of the sensor resolution was performed using a calibrated sensor with the linear range of 8500psi. The sensor was exposed to the atmosphere where the pressure reading from the sensor should be zero. The data from the SCIIB system was sampled at a rate of 50 samples per second for one minute, which should be high enough compared to the system's frequency response of 15Hz. The pressure measurement outputs within the one-minute sampling period are plotted in Figure 7-17. The standard deviation of the pressure data within this time period was calculated to be $\sigma=0.121$ psi. Therefore the resolution of the sensor system was estimated to be $2\sigma=0.242$ psi. The normalized resolution with respect to the dynamic range of the system was 0.003% of the full scale.

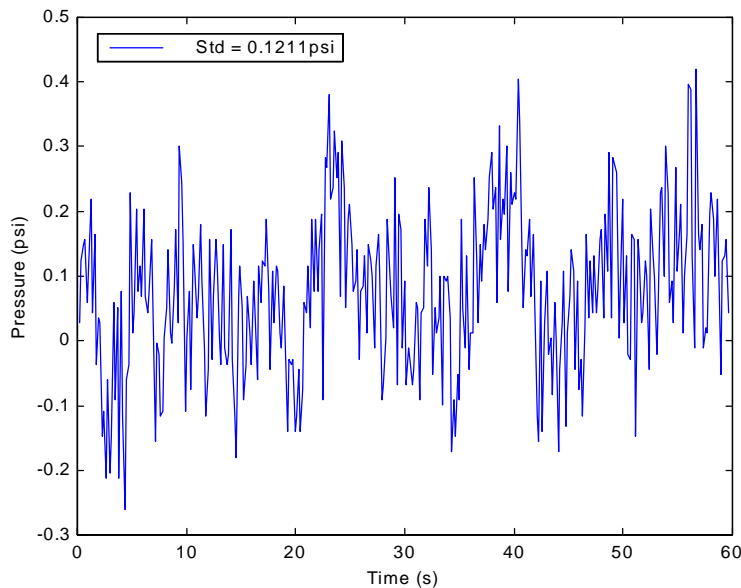


Figure 7-17. Standard deviation measurement of the SCIIB pressure sensor

It must be pointed out that the resolution of the sensor is not constant within the entire operating range due to the non-linear nature of the interference signal. However, by confining the operating range of the SCIIB sensor within its semi-linear range of an interference fringe, the resolution of the system should be retained within 60% of the maximum resolution as defined by Equation (2-11).

7.5.4 Repeatability of pressure measurement

Repeatability of the sensor can be measured by applying pressure to a certain preset point repeatedly only from one direction (increasing or decreasing). The largest difference of the sensor output readings can be used to specify the repeatability of the sensor. The same calibrated single-mode sensor was used to evaluate the repeatability of the system. Using the *APP* system, two consecutive measurements up to the full operating range of the sensor were performed with the results shown in Figure 7-18. For comparison purposes, the original calibration data is also shown. The deviation of the two measurement results with respect to the calibration data are plotted in Figure 7-19.

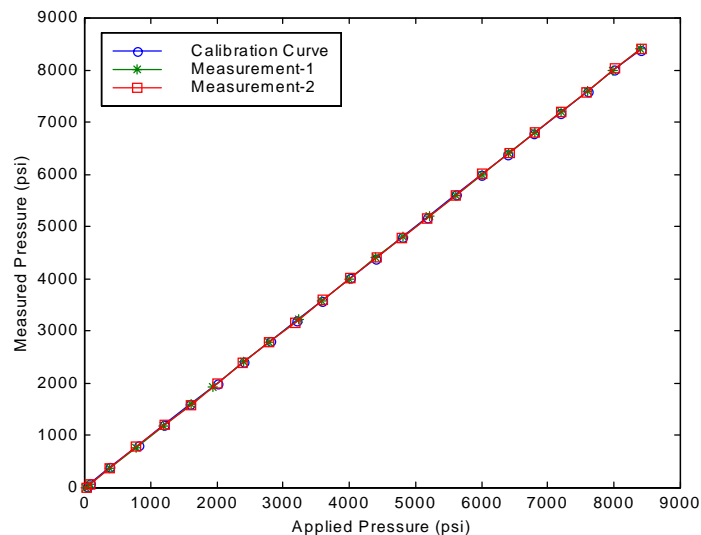


Figure 7-18. Repeatability test result of the pressure measurement

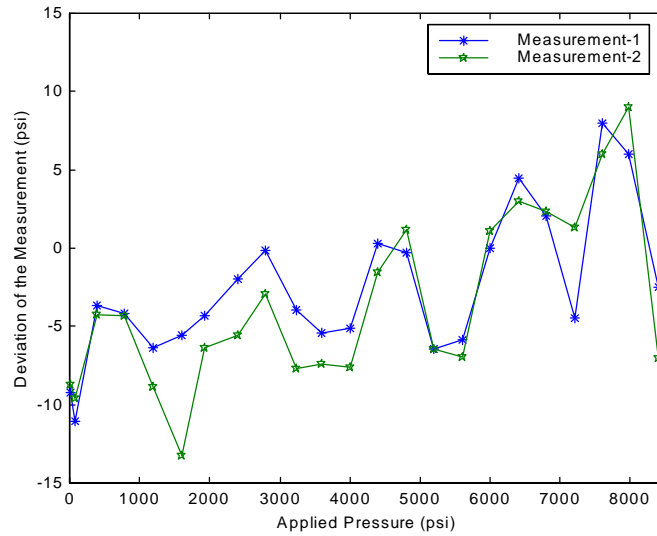


Figure 7-19. Deviation of the measured pressure with respect to the calibration data

As shown in Figure 7-19, the maximum deviation between the measured pressure and the calibrated pressure was within ± 13 psi. The normalized repeatability of the sensor system with respect to its dynamic range was therefore $\pm 0.15\%$ of the full scale.

7.5.5 System stability test

The same single-mode sensor with the operating range of 8500psi was also used to test the system stability. The sensor was kept in the pressure test chamber of the *APP* system for 24 hours starting from 4:00pm in the afternoon. The pressure of the chamber was maintained to the atmosphere pressure. The data acquisition system was programmed to sample the sensor's output every 20 seconds. The test result is shown in Figure 7-20. By processing the data, the maximum peak-to-peak pressure variation within the 24-hour time period was 3.3 psi. The normalized maximum variation was thus 0.04% of the full dynamic range. The test results also showed that the variation of the data was not unidirectional.

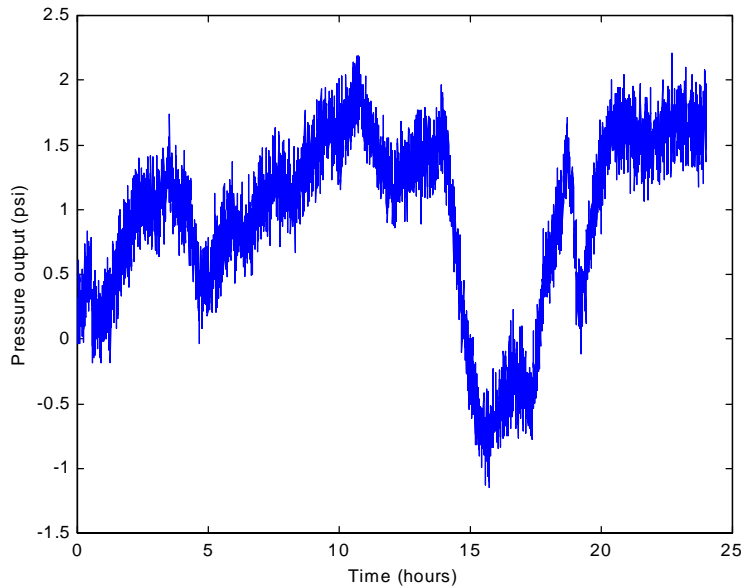


Figure 7-20. System stability test over 24 hours

It must be said that the complete evaluation of the system stability needs much longer test period (for example, one year). Therefore, the stability test result of 24-hour period was hence not quite conclusive.

7.5.6 Temperature cross-sensitivity of pressure measurement

The cross sensitivity to temperature could result in errors of the pressure measurement when the environmental temperature changes. The construction of the APP pressure calibration system allowed us to characterize the temperature cross sensitivity of the SCIIB pressure sensor by measuring pressures at different elevated temperatures. As shown in Figure 7-21, the same single-mode fiber sensor with the dynamic range of 8500psi was tested at temperatures of 24°C, 88°C, and 206°C respectively. Figure 7-22 shows clearly the measurement errors at the two elevated temperatures. The maximum deviation was 215psi at 88°C and 307psi at 206°C respectively. The maximum temperature cross sensitivity was thus calculated to be 0.04% per degree Celsius.

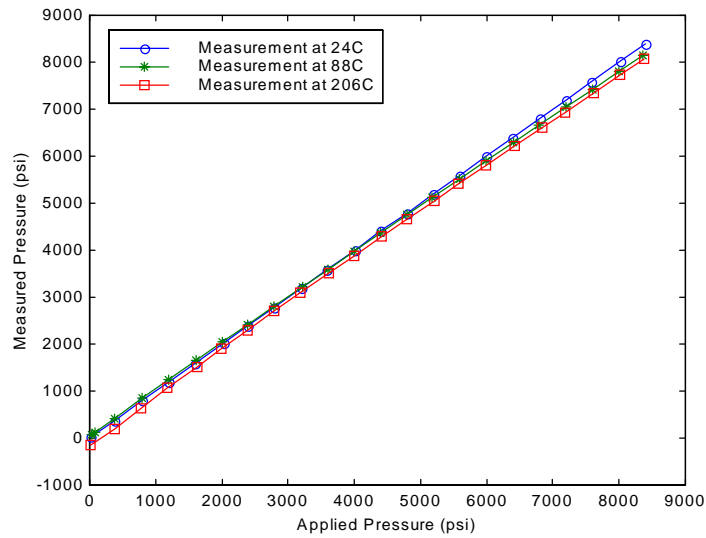


Figure 7-21. Temperature cross sensitivity test of the SCIIB pressure sensor

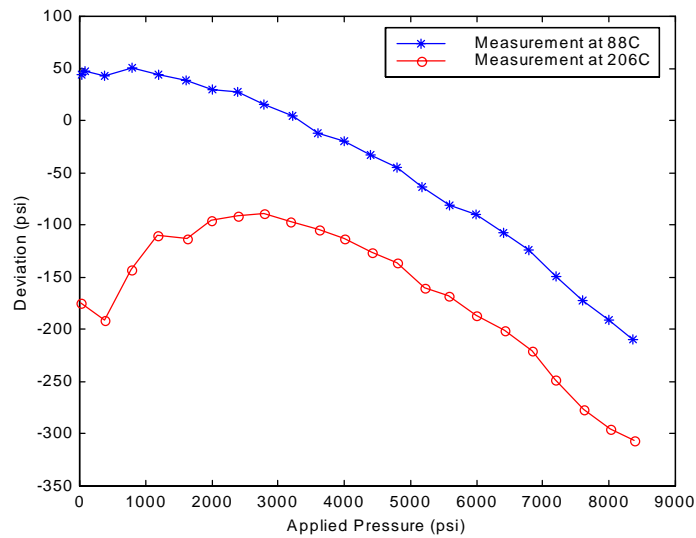


Figure 7-22. Pressure measurement errors resultant from the temperature dependence

It was also noticed that the large errors were found at the low and high pressure range where the nonlinear effects became the largest. The temperature cross sensitivity could thus be reduced by sacrificing the dynamic range of the sensor.

7.5.7 Overpressure capability test

In real downhole applications, pressures higher than the nominal values might be encountered due to the use of steam flood to pump the oil to the surface. It is therefore very important for the sensor to be able to sustain burst pressures higher than its dynamic range. The overpressure capability of the SCIIB pressure sensors was thus tested. The sensor used in the overpressure tests was a multimode fiber-based sensor with a gauge length of 1.0mm, an initial cavity length of 5.67 μ m, and a fringe visibility of 49%. The sensor was calibrated to have a dynamic range of 1800psi.

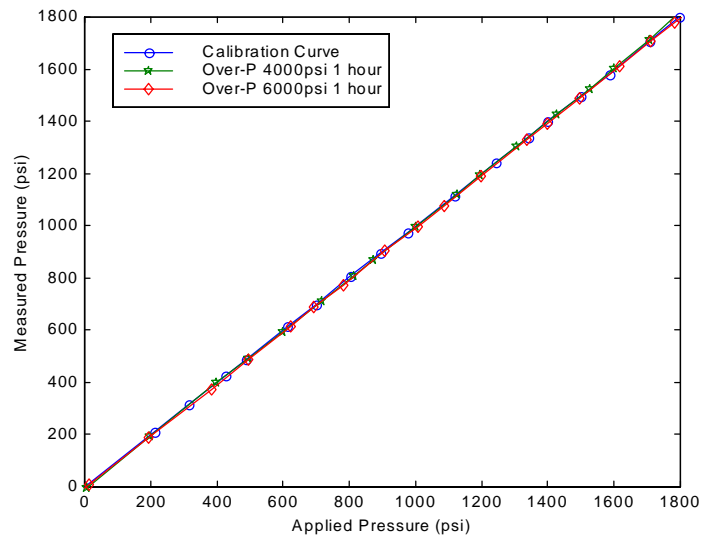


Figure 7-23. Overpressure test results of the multimode SCIIB sensor

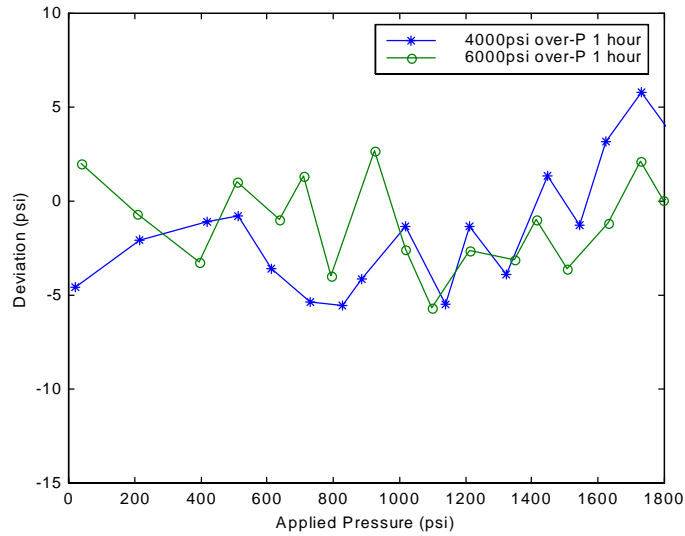


Figure 7-24. Sensor deviation of the overpressure tests

The over pressure tests were conducted at room temperatures. The sensor was first over pressured to 4000psi and kept in the pressurized chamber for one hour. After the pressure was released, the sensor was evaluated to measure pressures within its dynamic range. The same experiment was also conducted at an overpressure of 6000psi for one hour. The experimental results are shown in Figure 7-23. The deviations after the overpressures from the original calibration line are shown in Figure 7-24. As shown in Figure 7-24, the overpressures do not show any observable effect on the sensor performance. The deviations shown in Figure 7-24 are within the range governed by the repeatability of the sensor.

7.5.8 Dynamic pressure measurement

To demonstrate the sensor’s dynamic response, the calibrated SCIIB pressure sensors were applied for dynamic pressure measurements. The pressure signal was provided by the *APP* system after it was programmed to pressurize the chamber from atmosphere pressure to the preset pressure at even steps. Both the multimode sensor and the single-

mode sensor were tested. The multimode sensor used was the one with an operating range of 1800psi, and the single-mode sensor had an operating range of 8500psi. The testing range for the multimode sensor was 900psi and that for single-mode sensor was 8500psi.

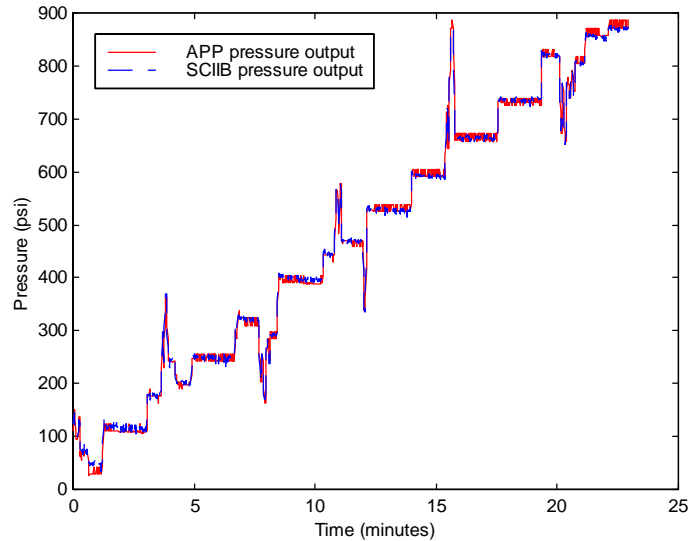


Figure 7-25. Dynamic pressure measurement results of the multimode sensor

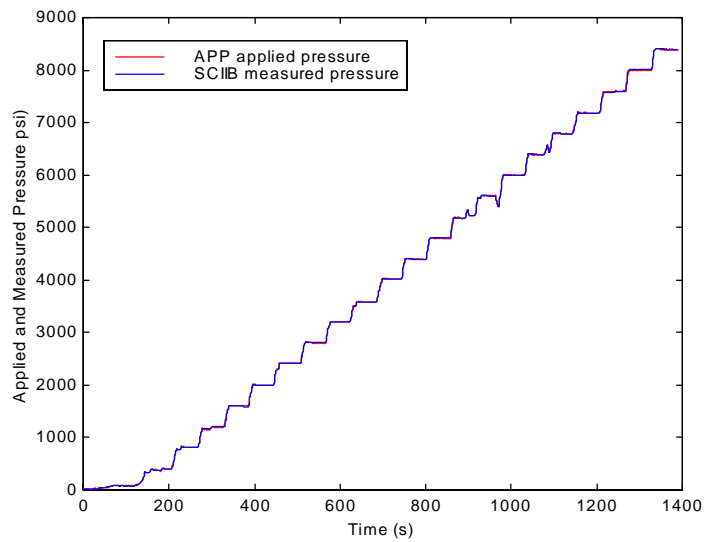


Figure 7-26. Dynamic pressure measurement results of the single sensor

The pressure increases measured by the SCIIB pressure sensors are shown in Figure 7-25 and Figure 7-26, for the multimode and single-mode fiber sensors respectively. The sampling rates of both the SCIIB sensor systems and the pressure gauge were set to one sample per second. The output of the built-in pressure gauge of the APP system is also plotted for comparison purposes. As shown in the two figures, the measurement results of both the multimode and single-mode fiber SCIIB sensors agreed very well with that of the built-in pressure gauge.